

Optimizing Machinability in Wire EDM of AISI P20 Steel Employing Composite Material Wires with Hybrid Neural Network Approach

B. Kiran Kumar^{1,*}, K. Siva Satya Mohan², K. Venkatesan³, K. Tilak⁴

Abstract

AISI P20+Ni steel is extensively used for forging dies, plastic moulds, and automotive die components due to its excellent polishability, hardness, and homogeneity. This research utilizes Wire Electrical Discharge Machining (WEDM) to process pre-hardened AISI P20+Ni steel, focusing on minimizing both recast layer thickness (RLT) and kerf width (KW). The performance of wires made from composite materials, including zinc-coated brass wire (ZBW), cryogenically treated ZBW (CZBW), and ultrasonic vibration-assisted brass wire (UVBW), is evaluated in this study. Pulse on time (T_{ON}), pulse off time (T_{OFF}), peak current (I_P), and servo voltage (V_S) are the main machining parameters considered during experiments. Their effects on RLT and KW are studied experimentally, and the process was additionally enhanced through the application of Response Surface Methodology and the Search and rescue algorithm (SAR). Results show that UVBW yields the best performance, Utilizing optimized parameters of T_{ON} at 110 μ s, T_{OFF} at 60 μ s, I_P of 12 A, and V_S set to 6 V, achieving a desirability of 0.722 in RSM. Additionally, a hybrid deep belief neural network integrated with SAR (DBN-SAR) is found to be the most accurate method for predicting WEDM outcomes, outperforming standalone DBN and RSM with RMSE values ranging from 0.024 to 0.03, indicating lower error.

Keywords: WEDM, AISI P20+Ni, optimization, hybrid modeling, Composite EDM Wires

INTRODUCTION

Wire Electric Discharge Machining (WEDM) is commonly employed to machine hard materials such as mold and die steels. As an advanced form of EDM, it attracts research aimed at enhancing machinability for better productivity and surface finish. Key challenges include minimizing Recast Layer Thickness (RLT) and Kerf Width (KW). Though tool wear is avoided, wire damage from debris remains a concern.

AISI P20 is a mold steel valued for polishability. Variants like AISI P20+S and P20+Ni enhance machinability and polishability. P20+Ni offers high purity, corrosion resistance, fine polish, and hardness (360–400 BHN) due to added 1% nickel content [1].

Kumar et al. [2] conducted a review of recent research on Wire Electrical Discharge Machining (WEDM), emphasizing how process parameters such as pulse duration, wire feed rate, dielectric pressure, and applied voltage influence outcomes like cutting depth, surface finish, and material removal rate (MRR). They recommended adaptive

*Author for Correspondence

B. Kiran Kumar

¹Associate Professor, Department of Mechanical Engineering, Koneru Lakshmaiah Education Foundation, Vaddeswaram, Andhra Pradesh, India

²Assistant Professor, Department of Mechanical Engineering, Aditya University, Surampalem, Andhra Pradesh, India

³Professor, Department of Automobile Engineering, Bharath Institute of Higher Education and Research, Chennai, Tamil Nadu, India

⁴Student, Department of Mechanical Engineering, Koneru Lakshmaiah Education Foundation, Vaddeswaram, Andhra Pradesh, India

Received Date: September 24, 2025

Accepted Date: November 03, 2025

Published Date: February 07, 2026

Citation: B. Kiran Kumar, K. Siva Satya Mohan, K. Venkatesan, K. Tilak. Optimizing Machinability in Wire EDM of AISI P20 Steel Employing Composite Material Wires with Hybrid Neural Network Approach. Journal of Polymer & Composites. 2026; 14(Special Issue 1): S1120–S1133.p.

wire feed control to prevent wire breakage. Kuo et al. [3] introduced a surface modification method using stacked assisting electrodes, achieving improved surface roughness and microhardness with optimized parameters. Yuan et al. [4] applied Gaussian Process Regression to optimize high-speed WEDM, enhancing MRR and surface finish with reduced result variance. Abdulkareem et al. [5] compared dry and wet WEDM, finding wet WEDM superior due to less debris adhesion, which affects surface quality. Singh et al. [6] used RSM Box Behnken design on Al6063 and found pulse on time most significantly increased MRR, while other parameters had varying inverse effects.

Electrodes play a crucial role in WEDM performance. Joshi et al. [7] found copper electrodes effective in drilling Ti-6Al-4V, with T_{ON} affecting MRR and I_p influencing electrode wear. Mahapatra et al. [8] used square copper electrodes and optimized parameters using multi-criteria optimization technique -Technique for Order Preference by Similarity to Ideal Solution (TOPSIS) for improved MRR and surface finish in AISI P20. Sen et al. [9] showed silver-coated brass wires performed better than brass in maraging steel machining. Cryogenically treated brass and zinc-coated wires enhanced MRR and accuracy, as noted by Singh and Goyal [10]. Priyadarshini [11] found sub-cooled metals yielded better surface finish and MRR. According to Tosun [12], tool wear is significantly affected by changes in pulse duration and voltage. Chalisgaonkar [13] showed zinc-coated wires outperform uncoated ones. Ugrasen [14] confirmed molybdenum wire reduces electrode wear in SS304 machining. Overall, electrode type and process parameters significantly influence WEDM outcomes like surface roughness, MRR, and tool wear, with hybrid and treated wires offering improved performance.

Bharathi et al. [15] investigated how wire feed rate, pulse on/off durations, and voltage influence the SR and MRR of SS304, employing the Taguchi technique combined with multi-objective optimization. Optimal parameters were 60V, 4 μ s pulse times, and 5m/min wire speed. Choudhuri et al. [16] optimized SS316 machining with ANN-PSO, finding higher pulse on time increases SR and RLT. Gowthaman et al. [17] analyzed AISI4340, noting T_{ON} and S_v increase MRR and SR, while higher pulse off time improves surface finish. Kuruvila and Ravindra [18] combined Taguchi and genetic algorithms for hot die steel, recommending lower pulse off time for better performance and higher pulse on time for increased MRR.

The advancement of computers enabled the integration of machine learning into optimization for improved process parameters. Singh and Misra [19] used half-hard brass wire to machine Nimonic 263 and observed that pulse on/off times significantly affected surface roughness, which was validated through an artificial neural network (ANN). Nayak and Mahapatra [20] applied a hybrid ANN-bat algorithm to improve taper machining of cryo-processed Inconel 718, using BPNN and Levenberg–Marquardt for performance prediction. Singh et al. [21] used ANN with a full factorial design to machine Al6063, achieving a prediction error of 3.898%. Chou et al. [22] predicted wire rupture in WEDM using ANN with 85% accuracy. Ulas et al. [23] used ELM and SVM to forecast surface roughness in Al7075, obtaining a 0.920 regression coefficient.

Previous studies have focused mainly on enhancing WEDM performance through adjustments in electrical and non-electrical parameters. However, limited work has explored the effect of different wire materials on machining mold tool steels. This research addresses that gap by evaluating the WEDM performance of AISI P20+Ni used in molding applications. Key performance indicators such as RLT and KW are evaluated using wires made from composite materials in Wire EDM, including zinc-coated brass wire (ZBW), cryogenically treated ZBW (CZBW), and ultrasonic vibration-assisted brass wire (UVBW).

METHODOLOGY

The research employed the eNOVA Electronic CNC WEDM machine from Electronica India Ltd., equipped with TURBO motion control for precise 5-axis CNC operation. Different types of wires,

including UVBW, ZBW, and CZBW, were employed for machining AISI P20+Ni steel, a material widely applied in plastic molding dies.

The methodology begins with WEDM machining, followed by parametric analysis using literature-based input and output parameters depicted in Figure 1. The Box-Behnken Design of Response Surface Methodology (RSM-BBD) is utilized for input optimization. A hybrid DBN with SAR algorithm (DBN-SAR) is developed to predict performance, and results are compared to evaluate model accuracy. Key parameters such as V_s , I_p , T_{OFF} , and T_{ON} significantly influenced performance metrics like radial land thickness (RLT) and kerf width (KW). A total of 27 experiments were conducted using RSM-BBD with three input parameter levels, as shown in Table 1.

RESULTS AND DISCUSSION

The input parameters and responses of WEDM performance are presented in Tables 2 and 3. Table 4 presents the effects of the selected input parameters. RLT reduces as T_{OFF} increases and when V_s , I_p , and T_{ON} decrease. Likewise, KW declines with lower values of T_{ON} , T_{OFF} , V_s , and I_p . Figure 2 presents the relationship between input factors and RLT in the machining of AISI P20+Ni. Among the electrode materials, UVBW achieves the lowest RLT, measuring 7.384 μm . KW is a critical indicator of product quality, with lower values signifying better machining performance. Figure 3 shows the effect of input factors on KW. UVBW again provides the lowest KW among the electrode materials, reaching 0.246 mm.

Table 1. Coded input factors with their levels.

Input Factors	Unit	Level 1 (Low)	Level 2 (Medium)	Level 3 (High)
Pulse on Time	μS	100	105	110
Pulse off time	μS	50	55	60
Peak current	A	10	11	12
Servo voltage	V	4	5	6

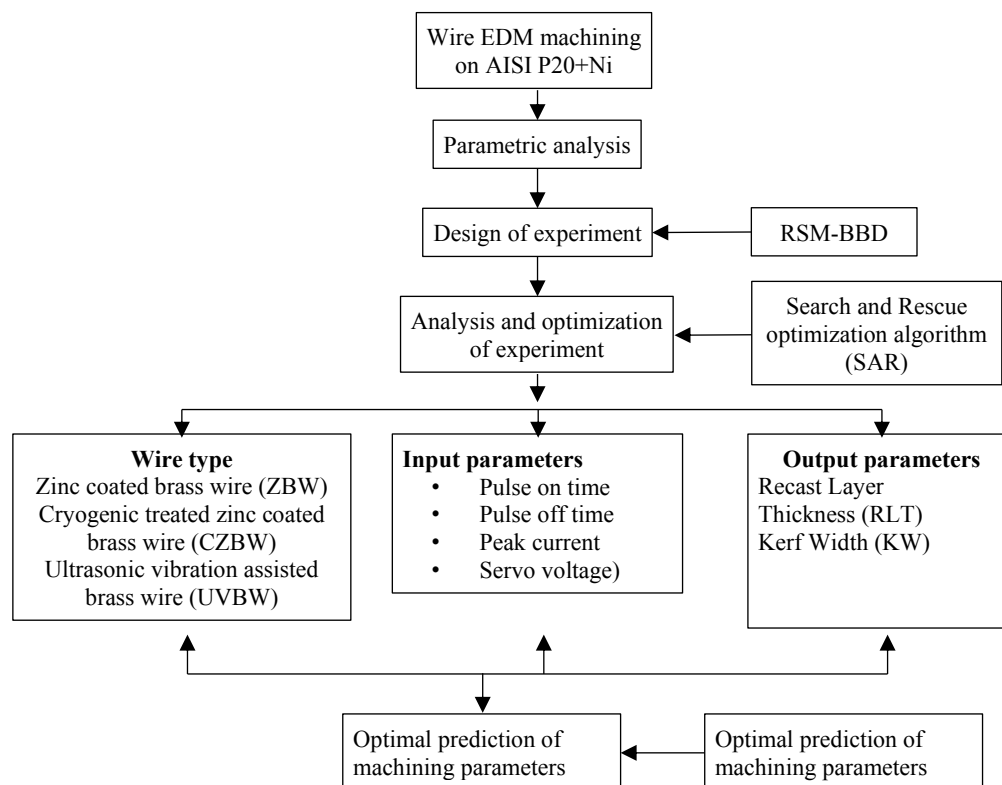


Figure 1. Workflow of the proposed methodology.

WEDM input parameters are optimized for AISI P20+Ni machining using different cutting wires, focusing on RLT and KW. Utilizing RSM design of experiment, input-output parameter relationships are explored. Analysis of Variance (ANOVA) reports validate the reliability of designed RSM models for diverse machining conditions. Tables 5-7 present ANOVA results for RLT response using ZBW, CZBW and UVBW respectively. ANOVA of the RSM models as given in Equations. (1) to (3) reveals significant RLT responses for ZBW, CZBW and UVBW in WEDM of AISI P20+Ni respectively:

$$RLT_1 = 8.53542 + 1.60833A - 1.14583B + 0.795833C - 0.195833D - 1.525AB + 1.05AC - 0.4AD - 0.875BC + 0.3125BD - 0.0875CD + 1.47083A^2 + 0.795833B^2 - 0.341667C^2 + 0.102083D^2 \quad (1)$$

$$RLT_2 = 8.48 + 1.82A - 1.17B + 0.8932C - 0.2059D - 1.69AB + 1.01AC - 0.4012AD - 1.10BC + 0.3023BD - 0.0575CD + 1.20A^2 + 0.6086B^2 - 0.1564C^2 + 0.1173D^2 \quad (2)$$

$$RLT_3 = 8.93 + 2.21A - 1.36B + 0.8435C - 1.74AB + 0.8740AC - 0.7445AD - 0.9355BC + 0.6252BD - 0.7445AD + 1.19A^2 + 0.5072B^2 - 0.4523C^2 + 0.3043D^2 \quad (3)$$

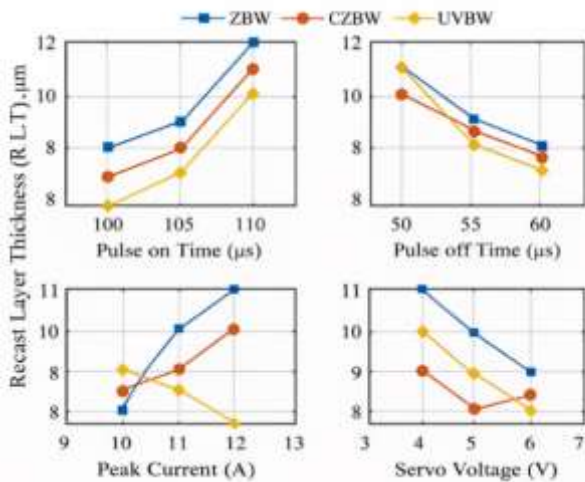


Figure 2. Effect of T_{ON} , T_{OFF} , I_P and V_S on RLT.

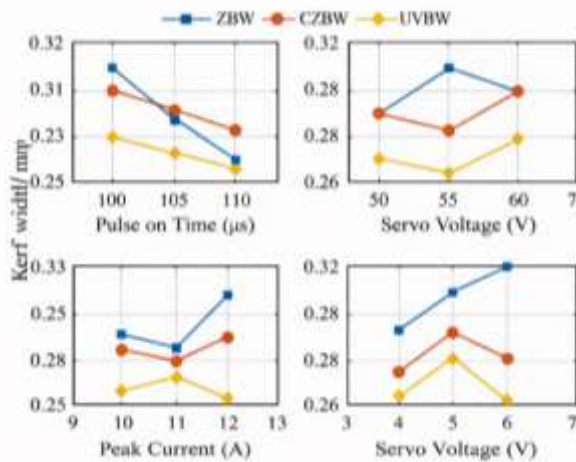


Figure 3. Effect of T_{ON} , T_{OFF} , I_P and V_S on KW.

Table 2. Experimental RLT outcomes during WEDM.

Run	T _{ON} (μs)	T _{OFF} (μs)	I _P (A)	V _s (V)	RLT (μm)		
					ZBW	CZBW	UVBW
1	100	50	11	5	9.7	8.25	8.221
2	110	50	11	5	16.6	16.517	16.102
3	100	60	11	5	8.9	8.16	8.73
4	110	60	11	5	9.7	9.465	9.664
5	105	55	10	4	9	9.2	8.903
6	105	55	12	4	10.3	10.68	10.514
7	105	55	10	6	8.1	8.12	7.384
8	105	55	12	6	8.7	8.68	8.521
9	100	55	11	4	8.4	8.26	8.21
10	110	55	11	4	14.7	14.59	14.317
11	100	55	11	6	8.3	8.16	8.035
12	110	55	11	6	11.4	11.28	11.164
13	105	50	10	5	8.5	8.421	8.371
14	105	60	10	5	8.2	8.03	7.906
15	105	50	12	5	12.1	11.12	11.942
16	105	60	12	5	8.3	8.092	7.735
17	100	55	10	5	7.9	7.761	7.384
18	110	55	10	5	9.3	9.627	9.897
19	100	55	12	5	8.3	7.921	7.623
20	110	55	12	5	13.9	13.843	13.632
21	105	50	11	4	12.9	12.709	12.647
22	105	60	11	4	8.8	8.751	8.537
23	105	50	11	6	9.8	9.69	9.621
24	105	60	11	6	8.2	8.15	8.012
25	105	55	11	5	8.6	8.73	8.935
26	105	55	11	5	9	8.752	8.935
27	105	55	11	5	8.9	8.914	8.935

RLT standardized residuals are close enough to the normal probability line as shown in Figure 4.

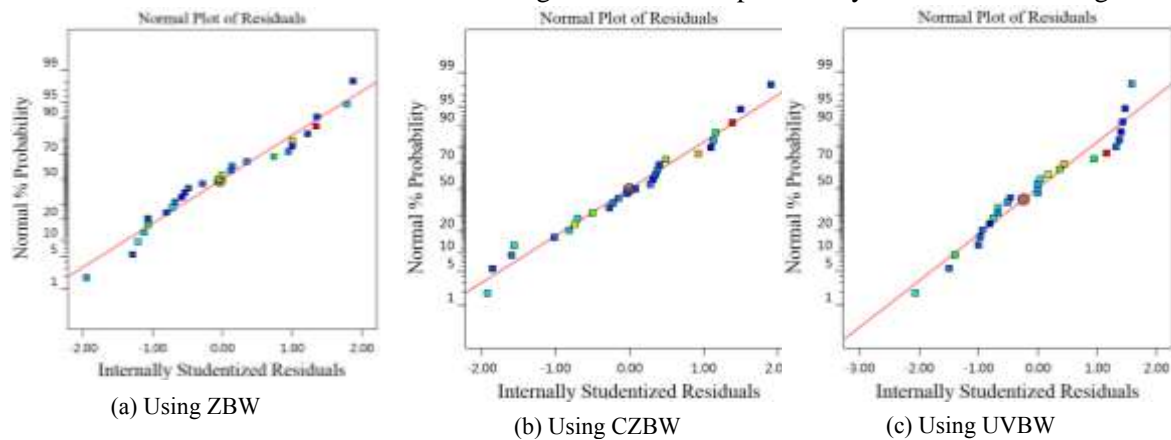


Figure 4. RLT normal probability plots obtained from RSM models.

From the Tables 8-10, Significant factors include A, B, C and interactions AB, BC, A², B² and C², with low p-values, implying their impact on the response. High R² values, indicating excellent model fits.

$$KW_1 = 0.3065 - 0.0141A + 0.0044B - 0.0111C + 0.0024D - 0.0133AB - 0.0095AC - 0.0016AD - 0.0122BC - 0.0042BD - 0.0019CD + 0.0063A^2 - 0.0072B^2 - 0.0133C^2 - 0.0004D^2 \dots\dots\dots (1)$$

$$KW_2 = 0.2922 - 0.0111A + 0.0016B - 0.0060C - 0.0004D - 0.0168AB - 0.0043AC + 0.0003AD - 0.0018BC - 0.0011BD + 0.0006CD - 0.0019A^2 + 0.0045B^2 + 0.0108C^2 - 0.0009D^2 \dots\dots\dots (2)$$

Table 3. Experimental KW outcomes during WEDM.

Run	TON (µs)	TOFF (µs)	IP (A)	Vs (V)	KW (mm)		
					ZBW	CZBW	UVBW
1	100	50	11	5	0.296	0.289	0.275
2	110	50	11	5	0.299	0.294	0.284
3	100	60	11	5	0.338	0.334	0.328
4	110	60	11	5	0.288	0.272	0.267
5	105	55	10	4	0.297	0.295	0.246
6	105	55	12	4	0.324	0.304	0.259
7	105	55	10	6	0.319	0.297	0.276
8	105	55	12	6	0.311	0.311	0.257
9	100	55	11	4	0.312	0.29	0.252
10	110	55	11	4	0.297	0.267	0.267
11	100	55	11	6	0.327	0.301	0.278
12	110	55	11	6	0.299	0.28	0.265
13	105	50	10	5	0.271	0.297	0.274
14	105	60	10	5	0.318	0.304	0.278
15	105	50	12	5	0.327	0.31	0.295
16	105	60	12	5	0.325	0.31	0.291
17	100	55	10	5	0.312	0.298	0.278
18	110	55	10	5	0.301	0.289	0.266
19	100	55	12	5	0.358	0.318	0.294
20	110	55	12	5	0.309	0.292	0.269
21	105	50	11	4	0.268	0.288	0.253
22	105	60	11	4	0.299	0.294	0.288
23	105	50	11	6	0.301	0.293	0.282
24	105	60	11	6	0.298	0.29	0.278
25	105	55	11	5	0.302	0.294	0.281
26	105	55	11	5	0.304	0.291	0.279
27	105	55	11	5	0.305	0.29	0.276

Table 4. Influence of input parameters.

Output response	Required effect	Input parameters			
		TON (µs)	TOFF (µs)	IP (A)	Vs (V)
RLT	↓	↓	↑	↓	↓
KW	↓	↓	↓	↓	↓

Table 5. ANOVA for RLT using ZBW ($R^2 = 0.9692$).

Source	Sum of Squares	df	Mean Square	F-value	p-value	Significant
Model	129.37	14	9.24	26.99	< 0.0001	✓
A – Pulse on time	17.74	1	17.74	51.8	< 0.0001	✓
B – Pulse off time	9	1	9	26.29	0.0003	✓
C – Peak current	4.34	1	4.34	12.68	0.0039	✓
D – Servo voltage	0.5664	1	0.5664	1.65	0.2227	–
AB	9.3	1	9.3	27.17	0.0002	✓
AC	4.41	1	4.41	12.88	0.0037	✓
AD	2.56	1	2.56	7.48	0.0181	✓
BC	3.06	1	3.06	8.94	0.0113	✓
BD	1.56	1	1.56	4.56	0.054	–
CD	0.1225	1	0.1225	0.3577	0.5609	–
A ²	11.54	1	11.54	33.69	< 0.0001	✓
B ²	3.38	1	3.38	9.86	0.0085	✓
C ²	0.6226	1	0.6226	1.82	0.2024	–
D ²	0.8893	1	0.8893	2.6	0.133	–
Residual	4.11	12	0.3424	–	–	–
Lack of Fit	4.02	10	0.4022	9.28	0.1011	Not significant
Pure Error	0.0867	2	0.0433	–	–	–
Cor Total	133.48	26	–	–	–	–

Table 6. ANOVA for RLT using CZBW ($R^2 = 0.9881$).

Source	Sum of Squares	df	Mean Square	F-value	p-value	Significant
Model	139.96	14	10.00	71.34	< 0.0001	✓
A – Pulse on time	22.62	1	22.62	161.41	< 0.0001	✓
B – Pulse off time	9.34	1	9.34	66.63	< 0.0001	✓
C – Peak current	5.47	1	5.47	39.03	< 0.0001	✓
D – Servo voltage	0.6260	1	0.6260	4.47	0.0562	–
AB	11.43	1	11.43	81.57	< 0.0001	✓
AC	4.11	1	4.11	29.35	0.0002	✓
AD	2.58	1	2.58	18.38	0.0011	✓
BC	4.86	1	4.86	34.66	< 0.0001	✓
BD	1.46	1	1.46	10.43	0.0072	✓
CD	0.0529	1	0.0529	0.3775	0.5504	–
A ²	7.64	1	7.64	54.54	< 0.0001	✓
B ²	1.98	1	1.98	14.10	0.0027	✓
C ²	0.1305	1	0.1305	0.9311	0.3536	–
D ²	1.17	1	1.17	8.37	0.0135	✓
Residual	1.68	12	0.1401	–	–	–
Lack of Fit	1.66	10	0.1661	16.45	0.0586	Not significant
Pure Error	0.0202	2	0.0101	–	–	–
Cor Total	141.64	26	–	–	–	–

Tables 8, 9 and 10 show the ANOVA results for KW response from ZBW, CZBW and UVBW models as follows:

Table 7. ANOVA for RLT using UVBW ($R^2 = 0.9962$).

Source	Sum of Squares	df	Mean Square	F-value	p-value	Significant
Model	133.65	14	9.55	222.11	< 0.0001	✓
A – Pulse on time	58.84	1	58.84	1369.08	< 0.0001	✓
B – Pulse off time	22.2	1	22.2	516.4	< 0.0001	✓
C – Peak current	8.54	1	8.54	198.65	< 0.0001	✓
D – Servo voltage	9	1	9	209.34	< 0.0001	✓
AB	12.07	1	12.07	280.71	< 0.0001	✓
AC	3.06	1	3.06	71.09	< 0.0001	✓
AD	2.22	1	2.22	51.58	< 0.0001	✓
BC	3.50	1	3.50	81.45	< 0.0001	✓
BD	1.56	1	1.56	36.38	< 0.0001	✓
CD	0.0562	1	0.0562	1.31	0.2753	–
A ²	7.60	1	7.60	176.77	< 0.0001	✓
B ²	1.37	1	1.37	31.92	0.0001	✓
C ²	1.09	1	1.09	25.39	0.0003	✓
D ²	0.4938	1	0.4938	11.49	0.0054	✓
Residual	0.5158	12	0.043	–	–	–
Lack of Fit	0.5158	10	0.0516	–	–	–
Pure Error	0	2	0	–	–	–
Cor Total	134.17	26	–	–	–	–

Table 8. ANOVA for KW using ZBW ($R^2 = 0.9663$).

Source	Sum of Squares	df	Mean Square	F-value	p-value	Significant
Model	0.0094	14	0.0007	24.61	< 0.0001	✓
A-Pulse on time	0.0014	1	0.0014	50.26	< 0.0001	✓
B-Pulse off time	0.0001	1	0.0001	4.91	0.0467	✓
C-Peak current	0.0008	1	0.0008	31.18	0.0001	✓
D-Servo voltage	0.0001	1	0.0001	3.06	0.1057	-
AB	0.0007	1	0.0007	25.80	0.0003	✓
AC	0.0004	1	0.0004	13.26	0.0034	✓
AD	0.0000	1	0.0000	1.55	0.2366	-
BC	0.0006	1	0.0006	22.05	0.0005	✓
BD	0.0003	1	0.0003	10.62	0.0069	✓
CD	0.0001	1	0.0001	2.07	0.1761	-
A ²	0.0002	1	0.0002	7.65	0.0171	✓
B ²	0.0003	1	0.0003	10.30	0.0075	✓
C ²	0.0009	1	0.0009	34.40	< 0.0001	✓
D ²	0.0000	1	0.0000	0.6000	0.4536	-
Residual	0.0003	12	0.0000	-	-	-
Lack of Fit	0.0003	10	0.0000	13.80	0.0694	not significant
Pure Error	4.667E-06	2	2.333E-06	-	-	-
Cor Total	0.0097	26	-	-	-	-

Table 9. ANOVA for KW using CZBW ($R^2 = 0.9358$).

Source	Sum of Squares	df	Mean Square	F-value	p-value	Significant
Model	0.0044	14	0.0003	12.5	< 0.0001	✓
A-Pulse on time	0.0015	1	0.0015	61.19	< 0.0001	✓
B-Pulse off time	0.0001	1	0.0001	3.6	0.082	-
C-Peak current	0.0004	1	0.0004	13.98	0.0028	✓
D-Servo voltage	0.0001	1	0.0001	3.82	0.0742	-
AB	0.0011	1	0.0011	44.56	< 0.0001	✓
AC	0.0001	1	0.0001	2.87	0.1161	-
AD	1.00E-06	1	1.00E-06	0.0397	0.8454	-
BC	0	1	0	0.4864	0.4988	-
BD	0	1	0	0.804	0.3875	-
CD	6.25E-06	1	6.25E-06	0.2481	0.6274	-
A ²	0	1	0	0.7444	0.4052	-
B ²	0.0001	1	0.0001	4.29	0.0606	-
C ²	0.0006	1	0.0006	24.47	0.0003	✓
D ²	0.0001	1	0.0001	2.78	0.1212	-
Residual	0.0003	12	-	-	-	-
Lack of Fit	0.0003	10	0	6.77	0.1354	not significant
Pure Error	8.67E-06	2	4.33E-06	-	-	-
Cor Total	0.0047	26	-	-	-	-

Table 10. ANOVA for KW using UVWB ($R^2 = 0.9253$).

I	Sum of Squares	df	Mean Square	F-Value	p-value	Significant
Model	0.0063	14	0.0005	10.62	0.0001	✓
A-Pulse on time	0.0007	1	0.0007	16.38	0.0016	✓
B-Pulse off time	0.0000	1	0.0000	0.2353	0.6364	-
C-Peak current	0.0000	1	0.0000	0.2518	0.6249	-
D-Servo voltage	0.0002	1	0.0002	5.61	0.0355	✓
AB	0.0015	1	0.0015	35.74	< 0.0001	✓
AC	0.0000	1	0.0000	0.9928	0.3387	-
AD	0.0002	1	0.0002	4.61	0.0530	-
BC	9.000E-06	1	9.000E-06	0.2115	0.6538	-
BD	0.0004	1	0.0004	8.94	0.0113	✓
CD	0.0003	1	0.0003	6.02	0.0304	✓
A ²	0.0000	1	0.0000	0.6582	0.4330	-
B ²	0.0005	1	0.0005	10.82	0.0065	✓
C ²	0.0002	1	0.0002	3.73	0.0773	-
D ²	0.0010	1	0.0010	24.42	0.0003	✓
Residual	0.0005	12	-	-	-	-
Lack of Fit	0.0005	10	0.0000	7.86	0.1180	not significant
Pure Error	0.0000	2	6.333E-06	-	-	-
Cor Total	0.0068	26	-	-	-	-

$$KW_3 = 0.2781 + 0.0101A + 0.0012B - 0.0012C - 0.0040D - 0.0195AB - 0.0032AC - 0.0035AD - 0.0015BC + 0.0049BD - 0.0040CD + 0.0023A^2 + 0.0093B^2 - 0.0055C^2 - 0.0035D^2 \quad (3)$$

KW standardized residuals are close enough to the normal probability line as shown in Figure 5 for ZBW, CZBW and UVBW models.

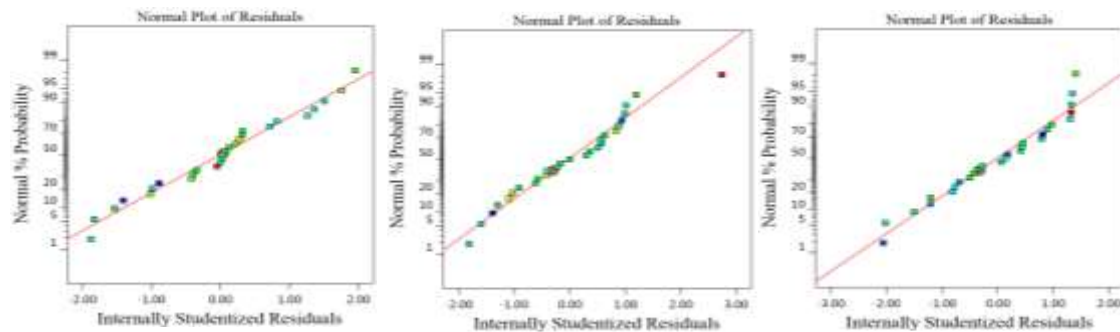


Figure 5. KW normal probability plots obtained from ZBW (Left), CZBW (Middle) and UVBW (Right) RSM models.

The Search and rescue (SAR) algorithm follows similar optimization criteria as RSM for RLT and KW. Optimal solutions from RSM and SAR models using ZBW, CZBW and UVBW data sets are provided in Table 11. Desirability factors of 0.761, 0.720 and 0.722 from RSM for ZBW, CZBW and UVBW suggest over 70% reliable output responses. SAR took 85 to 105 iterations to reach optimum. Based on the output responses, UVBW consistently shows superior performance, delivering about 10–17% improvement over ZBW and CZBW tool wires. This confirms its suitability as the optimal tool wire for machining AISI P20+Ni using WEDM.

Confirmatory analysis

RSM and SAR provided nearly similar optimum solutions, validated through actual experiments. Since the WEDM process on the eNOVA CNC machine does not accept decimal-coded inputs (e.g., 108.789 μ s), optimized factors were normalized to the nearest whole number (Table 12). Experiments were repeated thrice, and average outputs confirmed the results. Both methods yielded close outcomes with acceptable deviations, but SAR outperformed RSM in efficiency, accuracy, and simplicity. The highest deviation (-0.074) occurred in RSM, while SAR achieved minimal deviation (-0.002). Hence, SAR is identified as the more reliable optimization method for WEDM process parameter tuning.

WEDM prediction results from RSM-BBD and DBN-SAR models

The study aims to enhance prediction models for WEDM output with less training data. It assesses the prediction accuracy of RSM-BBD and hybrid Deep Belief Neural Network (DBN-SAR) models through experimentation. With 27 experiments per wire type, the models are trained and validated using experimental data, to prevent overfitting, 20% of the data was randomly chosen for validation, while the rest was allocated for training.

Table 13 displays predicted RLT and KW values via DBN-SAR and RSM-BBD models for experiment numbers using ZBW, CZBW and UVBW training data, reflecting machining outcomes with various brass wire types. Comparative analysis between DBN-SAR, RSM and normal DBN models is conducted. DBN-SAR's found to be in close alignment with the experimental results, indicating enhanced DBN performance. RSM's prediction accuracy is relatively lower. The reliability of RSM and DBN-SAR is assessed via regression analysis.

Figure 6 and 7 show the regression analysis results of DBN-SAR, with optimal results from UVBW data. The overall regression of the two parameters, namely RLT and KW are noticed as 0.9849, and 0.9934. Such overall regressions above 0.98 represent the learning process of developed DBN-SAR is accurate for performance forecasting. Therefore, the DBN-SAR method is selected as a suitable WEDM process prediction method than RSM and normal DBN methods.

The research evaluates the accuracy of the prediction model by calculating the root mean square error (RMSE). RMSE analysis, depicted in Figure 8, highlights DBN-SAR's superiority over normal DBN and RSM methods. DBN-SAR yields significantly lower RMSE values (0.03), indicating better

predictions compared to RSM (0.44). DBN's RMSE ranges from 0.25-0.32, while RSM's ranges from 0.39-0.44, both higher than DBN-SAR's values (0.024-0.03). DBN-SAR proves to be a more efficient prediction method compared to DBN and RSM, based on performance evaluations.

Table 11. Optimized input parameters from ZBW, CZBW and UVBW RSM, SAR models and their output responses

Model	Wire Type	Optimized input factors				Optimized output responses	
		$T_{ON}(\mu s)$	$T_{OFF}(\mu s)$	$I_P(A)$	$S_V(V)$	$RLT(\mu m)$	$KW(mm)$
RSM	ZBW	109.221	59.999	11.853	6.000	9.551	0.282
	CZBW	109.782	59.997	11.926	6.000	9.481	0.278
	UVBW	109.990	59.999	12.000	6.000	9.278	0.233
SAR	ZBW	108.789	60.000	11.924	6.000	9.409	0.286
	CZBW	109.992	59.989	11.994	5.996	9.475	0.269
	UVBW	110.000	59.977	12.000	6.000	9.304	0.238

Table 12. Confirmatory analysis of optimized outcomes via experimentation.

Normalized input factors		$T_{ON}=110 \mu s; T_{OFF}=60 \mu s; I_P=12A; S_V=6V$		
Responses	$RLT(\mu m)$	$KW(mm)$	Type of tool wire	
Actual values	10.131	0.270	ZBW	
RSM optimized	10.100	0.279		
Deviation	-0.031	+0.009		
SAR optimized	10.141	0.268	CZBW	
Deviation	+0.01	-0.002		
Actual values	9.718	0.269		
RSM optimized	9.644	0.278	UVBW	
Deviation	-0.074	+0.009		
SAR optimized	9.689	0.273		
Deviation	-0.029	+0.004	UVBW	
Actual values	9.317	0.240		
RSM optimized	9.283	0.233		
Deviation	-0.034	-0.007	UVBW	
SAR optimized	9.310	0.238		
Deviation	-0.007	-0.002		

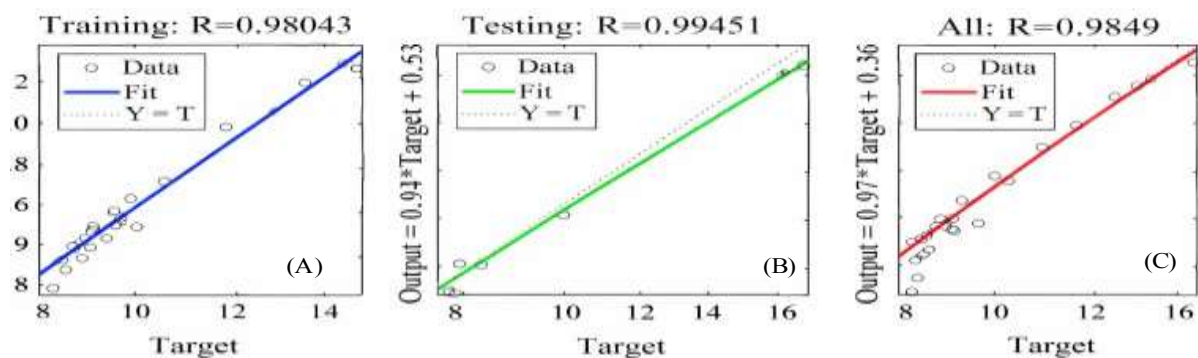


Figure 6. DBN-SAR regression analysis for RLT.

Table 13. RSM-BBD and DBN-SAR predictions using ZBW, CZBW and UVBW training data.

Ex. No.	ZBW				CZBW				UVBW			
	RLT		KW		RLT		KW		RLT		KW	
	RSM-BBD	DBN-SAR	RSM-BBD	DBN-SAR	RSM-BBD	DBN-SAR	RSM-BBD	DBN-SAR	RSM-BBD	DBN-SAR	RSM-BBD	DBN-SAR
1	9.02	9.62	0.29	0.30	8.17	8.32	0.29	0.29	8.69	8.25	0.27	0.28
2	16.09	16.68	0.30	0.30	15.98	16.58	0.30	0.30	16.52	16.13	0.30	0.28
3	9.16	8.81	0.34	0.34	8.61	8.08	0.33	0.34	9.20	8.75	0.32	0.33
4	10.12	9.77	0.29	0.29	9.66	9.38	0.27	0.27	10.10	9.70	0.27	0.27
5	8.64	9.09	0.29	0.29	8.93	9.27	0.29	0.30	9.37	8.93	0.24	0.28
6	10.76	10.38	0.33	0.32	11.06	10.77	0.30	0.31	10.95	10.54	0.26	0.26
7	7.39	8.03	0.31	0.32	7.39	8.21	0.30	0.30	7.79	7.42	0.27	0.28
8	8.81	8.62	0.33	0.37	9.07	8.76	0.31	0.31	8.99	8.55	0.26	0.22
9	8.70	8.31	0.31	0.31	8.33	8.18	0.30	0.29	8.69	8.24	0.26	0.26
10	14.32	14.63	0.29	0.29	14.37	14.53	0.27	0.26	14.76	14.35	0.26	0.27
11	8.70	8.24	0.33	0.33	8.17	8.10	0.30	0.30	8.47	8.07	0.29	0.28
12	11.12	11.47	0.30	0.30	11.00	11.22	0.28	0.28	11.57	11.19	0.26	0.27
13	8.99	8.42	0.28	0.31	8.67	8.48	0.30	0.29	8.82	8.39	0.28	0.27
14	7.82	8.13	0.32	0.32	7.93	8.10	0.31	0.30	8.36	7.94	0.28	0.27
15	12.50	12.17	0.33	0.33	12.77	11.03	0.31	0.31	12.35	11.97	0.28	0.29
16	7.84	8.22	0.32	0.33	7.63	8.16	0.31	0.31	8.23	7.76	0.29	0.29
17	8.12	7.99	0.31	0.31	7.69	7.84	0.30	0.29	7.83	7.42	0.28	0.28
18	10.04	9.37	0.31	0.30	10.09	9.71	0.29	0.29	10.33	9.93	0.27	0.27
19	7.79	8.24	0.36	0.33	7.56	8.00	0.32	0.32	8.04	7.65	0.29	0.29
20	13.90	13.83	0.31	0.31	14.02	13.77	0.29	0.30	14.07	13.65	0.27	0.27
21	12.92	12.83	0.27	0.27	12.83	12.64	0.29	0.29	13.06	12.67	0.25	0.26
22	8.75	8.87	0.31	0.30	8.68	8.81	0.30	0.29	8.98	8.57	0.28	0.29
23	10.07	9.73	0.30	0.30	9.86	9.76	0.30	0.29	10.03	9.64	0.28	0.28
24	8.40	8.13	0.30	0.30	8.13	8.07	0.30	0.29	8.48	8.04	0.28	0.28
25	8.83	8.67	0.30	0.30	8.80	8.79	0.29	0.29	9.39	8.96	0.28	0.28
26	8.83	8.92	0.30	0.30	8.80	8.84	0.29	0.29	9.42	8.96	0.28	0.28
27	8.83	8.82	0.30	0.31	8.80	8.84	0.29	0.29	9.40	8.96	0.28	0.27

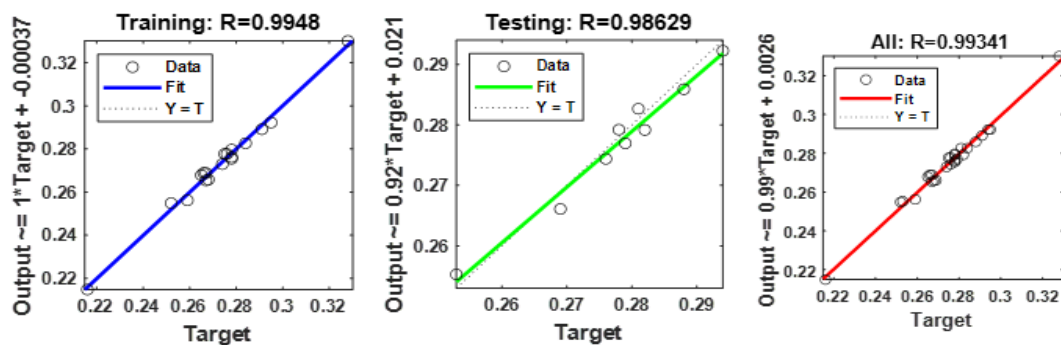


Figure 7. DBN-SAR regression analysis for KW.

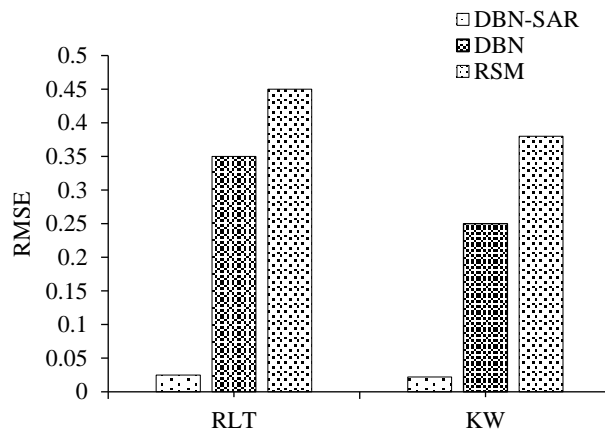


Figure 8. Analysis of RMSE obtained from RSM, DBN and DBN SAR models.

CONCLUSION

This research paper explores the machinability of AISI P20+Ni steel, widely used in die making, through Wire Electrical Discharge Machining (WEDM). The study reports a minimum Recast Layer Thickness (RLT) of 7.384 μm using ultrasonic vibration-assisted brass wire (UVBW), which is 5–7% lower than that achieved with zinc-coated brass wire (ZBW) and cryogenically treated ZBW (CZBW). UVBW also reduces kerf width (KW) by 8–10%, recording the lowest KW of 0.246 mm at specific settings, establishing it as the most effective tool wire for machining AISI P20+Ni using WEDM.

In WEDM optimization, T_{ON} , I_p , and V_s significantly affect RLT and KW, with Response Surface Methodology (RSM) models showing strong validity ($R^2 > 0.9$, $p < 0.0001$), and UVBW achieving optimal results of 9.278 μm RLT and 0.233 mm KW. Search and rescue algorithm (SAR) optimization for UVBW with 110 μs T_{ON} , 59.977 μs T_{OFF} , I_p 12A and V_s 6V, resulted in RLT of 9.304 μm and KW of 0.238 μm . Experiments confirmed close results for both methods, but SAR outperformed RSM in accuracy, efficiency, and simplicity, proving more reliable overall. The study improves WEDM output prediction using limited data, comparing RSM-BBD and DBN-SAR models. Experiments show DBN-SAR closely matches actual results, outperforming RSM, with reliability confirmed through regression analysis across different brass wire types. DBN-SAR exhibits superior prediction performance with low RMSE (0.024–0.03) and high overall regression coefficient (0.99341). DBN-SAR is the preferred prediction method, offering higher efficiency and accuracy while requiring less training data than RSM.

REFERENCES

1. Russo D, Urbicain G, Sánchez Egea A J, Simoncelli A and Martinez Krahmer D. Milling force model for asymmetric end-mills during high-feed milling on AISI-P20. *Materials and Manufacturing Processes*. 2021; 36(15), 1761–7p.
2. Kumar, Rajeev and Shankar Singh. Current research trends in wire electrical discharge machining: an overview. *International Journal on Emerging Technologies*. 2012; 3(1), 33–7p.
3. Kuo, Chunliang, Huanjiun Kao and Hao Wang. Novel design and characterisation of surface modification in wire electrical discharge machining using assisting electrodes. *Journal of Materials Processing Technology*. 2017; 244, 136–13p.
4. Yuan, Jin, Kesheng Wang, Tao Yu and Minglun Fang. Reliable multi-objective optimization of high-speed WEDM process based on Gaussian process regression. *International Journal of Machine Tools and Manufacture*. 2008; 48(1), 47–13p.
5. Abdulkareem, Suleiman, Ahsan Ali Khan and Zakaria Mohd Zain. Experimental investigation of machining parameters on surface roughness in dry and wet wire-electrical discharge machining. In *Advanced Materials Research*. Trans Tech Publications Ltd. 2011; 264, 831–5p.

6. Singh T, Misra J P and Singh B. Experimental Investigation of Influence of Process Parameters on MRR during WEDM of Al6063 alloy. *Materials Today: Proceedings*. 2017; 4(2), pp.2242–5p.
7. Ritesh Joshi, Gopal Zinzala, Nishit Nirmal, and Kishan Fuse. Multi-Response Optimization of EDM for Ti-6Al-4V Using Taguchi-Grey Relational Analysis;. In *Solid State Phenomena*. Trans Tech Publications Ltd. 2017; 266, 43–7p.
8. Mahapatra, K K, Tripathy S, Thatoi D N, and Mohapatra S. Multi-objective Optimization of AISI P-20 Tool Steel During Electrical Discharge Machining. In *Current Advances in Mechanical Engineering*. Springer Singapore. 2021; 919–8p.
9. Ruma Sen, Bikash Choudhuri, John Deb Barma, and Prasun Chakraborti. Study the impact of process parameters and electrode material on wire electric discharge machining performances. *Materials Today: Proceedings*, 2018; 5(2), 7552–8p.
10. Navjot Singh, Parlad Kumar, and Khushdeep Goyal. Effect of two different cryogenic treated wires in wire electrical discharge machining of AISI D3 die steel. *Journal of mechanical engineering*, 2013; 43(2), 54–p6.
11. Manisha Priyadarshini, Chandan Kumar Biswas, and Ajit Behera. Machining of sub-cooled low carbon tool steel by wire-EDM. *Materials and Manufacturing Processes*. 2019; 34(12), 1316-9p.
12. Nihat Tosun, and Can Cogun. An investigation on wire wear in WEDM; *Journal of materials processing technology*. 2003;134(3), 273–5p.
13. Rupesh Chalisgaonkar, and Jatinder Kumar. Multi-response optimization and modeling of trim cut WEDM operation of commercially pure titanium (CPTi) considering multiple user's preferences. *Engineering Science and Technology, an International Journal*. 2015; 18(2), 125–9p.
14. Ugrasen G, Singh M B, and Ravindra H V. Optimization of process parameters for SS304 in wire electrical discharge machining using Taguchi's technique. *Materials today: proceedings*. 2018; 5(1), 2877–6p.
15. Bharathi P, Tummalapenta Gouri Lalitha Priyanka, G. Srinivasa Rao, and B. Nageswara Rao. Optimum WEDM process parameters of SS304 using Taguchi method. *International Journal of Industrial and Manufacturing Systems Engineering*. 2016; 1(3), 69–3p.
16. Bikash Choudhuri, Ruma Sen, Subrata Kumar Ghosh, and S. C. Saha. Study of surface integrity and recast surface machined by Wire electrical discharge machining. *Materials Today: Proceedings*. 2018; 5(2), 7515–9p.
17. Gowthaman P S, Gowthaman J, and Nagasundaram N J M T P. A study of machining characteristics of AISI 4340 alloy steel by wire electrical discharge machining process. *Materials Today: Proceedings*. 2020; 27, 565–5p.
18. Nixon Kuruvila, and Ravindra H V. Parametric influence and optimization of wire EDM of hot die steel. *Machining Science and Technology*. 2011; 15(1), 47–28p.
19. Bhupinder Singh and J P Misra. Surface finish analysis of wire electric discharge machined specimens by RSM and ANN modelling. *Measurement*. 2019;137, 225–12p.
20. Bijaya Bijeta Nayak, and Siba Sankar Mahapatra. Optimization of WEDM process parameters using deep cryo-treated Inconel 718 as work material. *Engineering Science and Technology, an International Journal*. 2016; 19(1), 161–9p.
21. Singh T, Kumar P, and Misra J P. Modelling of MRR during Wire-EDM of ballistic grade alloy using artificial neural network technique. *Journal of Physics: Conference Series*. IOP Publishing. 2019; 1240(1), pp.012114.
22. Ping-Hsien Chou, Yean-Ren Hwang, and Bling-Hwa Yan. The study of machine learning for wire rupture prediction in WEDM. *The International Journal of Advanced Manufacturing Technology*. 2022; 119(1), 1301–10p.
23. Mustafa Ulas, Osman Aydur, Turan Gurgenc, and Cihan Ozel. Surface roughness prediction of machined aluminum alloy with wire electrical discharge machining by different machine learning algorithms. *Journal of Materials Research and Technology*. 2020; 9(6), 12512–12p.